Available online at www.sciencedirect.com
ScienceDirect
Journal of Power Sources 168 (2007) 251–257
JOURNAL OF POWER SOURCES
www.elsevier.com/locate/jpowsour

Effect of SiO_2-ZrO_2 supports prepared by a grafting method on hydrogen production by steam reforming of liquefied natural gas over Ni/SiO_2-ZrO_2 catalysts

Jeong Gil Seo, Min Hye Youn, In Kyu Song *

School of Chemical and Biological Engineering, Research Center for Energy Conversion and Storage, Seoul National University, Shinlim-dong, Kwanak-ku, Seoul 151-744, South Korea

Received 9 December 2006; accepted 22 February 2007
Available online 12 March 2007

Abstract

SiO_2-ZrO_2 supports with various zirconium contents are prepared by grafting a zirconium precursor onto the surface of commercial Carbosil silica. Ni(20 wt.%)/SiO_2-ZrO_2 catalysts are then prepared by an impregnation method, and are applied to hydrogen production by steam reforming of liquefied natural gas (LNG). The effect of SiO_2-ZrO_2 supports on the performance of the Ni(20 wt.%)/SiO_2-ZrO_2 catalysts is investigated. SiO_2-ZrO_2 prepared by a grafting method serves as an efficient support for the nickel catalyst in the steam reforming of LNG. Zirconia enhances the resistance of silica to steam significantly and increases the interaction between nickel and the support, and furthermore, prevents the growth of nickel oxide species during the calcination process through the formation of a ZrO_2-SiO_2 composite structure. The crystalline structures and catalytic activities of the Ni(20 wt.%)/SiO_2-ZrO_2 catalysts are strongly influenced by the amount of zirconium grafted. The conversion of LNG and the yield of hydrogen show volcano-shaped curves with respect to zirconium content. Among the catalysts tested, the Ni(20 wt.%)/SiO_2-ZrO_2 (Zr/Si = 0.54) sample shows the best catalytic performance in terms of both LNG conversion and hydrogen yield. The well-developed and pure tetragonal phase of ZrO_2-SiO_2 (Zr/Si = 0.54) appears to play an important role in the adsorption of steam and subsequent spillover of steam from the support to the active nickel. The small particle size of the metallic nickel in the Ni(20 wt.%)/SiO_2-ZrO_2 (Zr/Si = 0.54) catalyst is also responsible for its high performance.

Keywords: Silica-zirconia support; Nickel catalyst; Grafting method; Liquefied natural gas; Steam reforming; Hydrogen production

1. Introduction

The development of new and clean energy has been widely studied because of the high price of fossil fuels and associated environmental problems [1]. Hydrogen energy, therefore, has attracted considerable attention as a promising and clean energy source because of its potential applicability in fuel cell systems for the large-scale generation of electricity or for vehicle operation [2,3]. Several feasible routes for the production of hydrogen are available, including steam reforming, partial oxidation, and auto-thermal reforming of hydrocarbons [4–7]. Among these reforming reactions, steam reforming has been recognized as a suitable process for converting methane into hydrogen. Natural gas, which is mainly composed of methane, can be directly utilized as an alternate source for the production of hydrogen by steam reforming reaction. The extensive piping system for liquefied natural gas (LNG) in modern cities also makes this fuel well suited as a hydrogen source for residential reformers. Although the steam reforming of methane is an energy-intensive process because of its high endothermic nature, hydrogen-rich gas ($H_2/CO = 3$) can be produced by the steam reforming of methane, as follows:

$$CH_4 + H_2O \rightarrow CO + 3H_2 \quad \Delta H_{298\,K} = 206\,kJ\,mol^{-1} \qquad (1)$$

Nickel-based catalysts have been widely used in the steam reforming of methane. Although these are much cheaper than ruthenium- and rhodium-based catalysts, they require a high reaction temperature and an excess amount of steam to prevent

* Corresponding author. Tel.: +82 2 880 9227; fax: +82 2 889 7415.
E-mail address: inksong@snu.ac.kr (I.K. Song).

0378-7753/$ – see front matter © 2007 Elsevier B.V. All rights reserved.
doi:10.1016/j.jpowsour.2007.02.084

the sintering of nickel particles and the deposition of carbon on the catalyst surface [4,5,8]. Insufficient thermal and chemical stability of the supporting materials also contribute to deactivation of supported nickel catalysts [9]. Therefore, many attempts have been made to increase the stability of supported nickel catalysts by introducing second metals such as potassium, calcium, magnesium, cerium, and molybdenum [10–12], or by employing various supporting materials [13–15]. The performance of supported nickel catalysts in the steam reforming reaction depends not only on the nature and structure of the active nickel, but also on the chemical and textural properties of the supporting material. Thus, the modification of supporting materials for improving the catalytic performance of supported nickel catalysts in the steam reforming reaction is of interest.

Ni/SiO_2 catalysts have been widely investigated for use in many reactions [15–19]. It is known, however, that silica is readily aggregated by heating in the presence of steam [15]. Therefore, the direct use of silica as a supporting material in the steam reforming reaction has been restricted. This indicates that the low steam resistance of silica needs to be improved for the practical application of silica in the steam reforming process. It has been reported [20–23] that the addition of small amounts of zirconia increases the stability of silica and that a Ni/SiO_2-ZrO_2 catalyst shows a strong resistance against steam in the reforming reaction [15]. It has also been found [24] that the addition of zirconia to a nickel-based catalyst remarkably enhances the adsorption of steam onto its surface and activates the gasification of hydrocarbons or carbon precursors adsorbed on the catalyst surface during the steam reforming reactions. SiO_2-ZrO_2 can be synthesized by a sol–gel process [15,25–27], impregnation [28], co-precipitation [29], and grafting methods [30–33]. The chemical properties of SiO_2-ZrO_2 prepared by a grafting method are different from those obtained from other preparation routes [30–33]. Therefore, it is expected that SiO_2-ZrO_2 obtained by a grafting method will show interesting properties as a support for the nickel catalyst in the steam reforming of LNG.

In this work, a series of SiO_2-ZrO_2 supports with various zirconium contents were prepared by grafting a zirconium precursor onto the surface of SiO_2. Ni/SiO_2-ZrO_2 catalysts are then prepared by an impregnation method for use in hydrogen production by steam reforming of LNG. The effect of SiO_2-ZrO_2 supports on the performance of the Ni/SiO_2-ZrO_2 catalysts in the steam reforming of LNG is investigated.

2. Experimental

2.1. Preparation of SiO_2-ZrO_2 (SZ-X) support and Ni/SiO_2-ZrO_2 (Ni/SZ-X) catalyst

SiO_2-ZrO_2 supports with various zirconium contents were prepared by grafting an appropriate amount of zirconium precursor onto the surface of commercial silica (Carbosil), according to the similar method reported in the literature [30–33]. Fig. 1 shows a schematic of the procedure for the preparation of a SiO_2-ZrO_2 support by the grafting method. 3.2 g of silica (Carbosil) was uniformly dispersed in 100 ml of anhydrous toluene (Aldrich), and 0.6 ml of triethylamine (TEA, Fluka) was then added to the silica slurry to activate the hydroxyl groups on the silica surface. 2.4 g of zirconium precursor ($Zr(OBu)_4$, Aldrich) was slowly added to the slurry at a rate of 0.01 g min^{-1} with constant stirring, and the resulting slurry was stirred at room temperature for 6 h to achieve complete reaction of the activated surface hydroxyl groups of silica with the butoxide groups of zirconium precursor. After removing the unreacted zirconium precursor and butanol (by-product) by centrifugation, the slurry was washed several times with anhydrous toluene. Upon addition of an excess amount of deionized water to the washed slurry, a white gel was formed within a few seconds. After maintaining the white gel in deionized water for 6 h, the solid product was isolated by filtration. The solid product was dried overnight at 120 °C, and then calcined at 700 °C for 5 h to yield the SiO_2-ZrO_2 support. The prepared SiO_2-ZrO_2 support was denoted as SZ-X (X = 1, 2, 3, and 6), where X is the number of times the overall preparation process was repeated. For example, SZ-2 denotes an SiO_2-ZrO_2 support that was prepared by repeating the entire process twice (by adding 2.4 g of $Zr(OBu)_4$ twice through the entire preparation process).

The Ni/SiO_2-ZrO_2 catalysts were prepared by impregnating known amounts of a nickel precursor ($Ni(NO_3)_2{\cdot}6H_2O$, Aldrich) onto the Carbosil SiO_2 (SZ-0), SZ-1, SZ-2, SZ-3, and SZ-6 supports. The nickel loading was fixed at 20 wt.% in all cases. The prepared catalysts were denoted as Ni/SZ-X (X = 0, 1, 2, 3, and 6).

2.2. Characterization

The chemical compositions of the SiO_2-ZrO_2 (SZ-X) supports were determined by scanning electron microscopy–energy dispersive spectroscopy (SEM–EDS) analyses (JSM-840A). The crystalline phases of the supports and supported catalysts

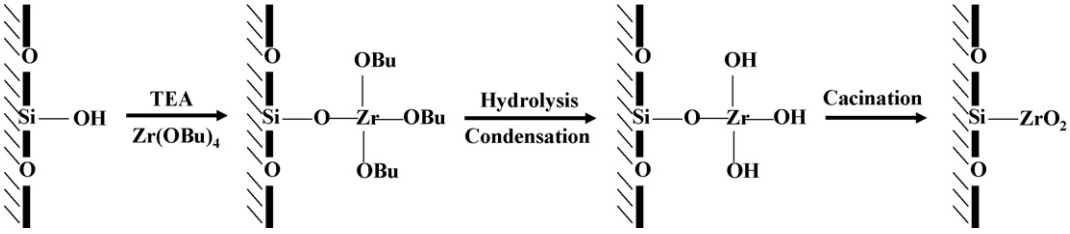

Fig. 1. Schematic of procedure for preparation of SiO_2-ZrO_2 support by grafting method.

were examined by X-ray diffraction (XRD: M18XHF-SRA, MAC Science) measurements using Cu Kα radiation (λ = 1.54056 Å) operated at 50 kV and 100 mA. The crystalline phases of the supports were also examined by Raman spectroscopy (HORIABA Jobin Yvon) analyses. In order to investigate the reducibility of the supported catalysts, temperature-programmed reduction (TPR) measurements were carried out in a conventional flow system with a moisture trap connected to a thermal conductivity detector (TCD) at temperatures ranging from room temperature to 1000 °C with a ramping rate of 5 °C min^{-1}. For the TPR measurements, a mixed stream of H_2 (2 ml min^{-1}) and N_2 (20 ml min^{-1}) was used for 0.1 g of catalyst sample.

2.3. Steam reforming of LNG

The steam reforming of LNG was carried out in a continuous flow fixed-bed reactor at atmospheric pressure. Each calcined catalyst (100 mg) was charged into a tubular quartz reactor, and was reduced with a mixed stream of H_2 (10 ml min^{-1}) and N_2 (30 ml min^{-1}) at 800 °C for 3 h. Water was sufficiently vaporized by passing a pre-heating zone and was continuously fed into the reactor together with LNG (92.0 vol.% of CH_4 and 8.0 vol.% of C_2H_6) and N_2 carrier (30 ml min^{-1}). The steam/carbon ratio in the feed stream was fixed at 2.0, and the total feed flow rate with respect to the catalyst was maintained at 27,000 ml h^{-1} g^{-1}. The catalytic reaction was carried out at 600 °C. The reaction products were periodically sampled and analyzed using an on-line gas chromatograph (Younglin, ACME 6000) equipped with a TCD. The conversion of LNG and the hydrogen yield were calculated according to the following equations on the basis of carbon balance.

$$\text{LNG conversion}\,(\%) = \left(1 - \frac{F_{CH_4,\,out} + F_{C_2H_6,\,out}}{F_{CH_4,\,in} + F_{C_2H_6,\,in}}\right) \times 100 \quad (2)$$

$$\text{Hydrogen yield}\,(\%) = \frac{F_{hydrogen,\,out}}{2 \times F_{CH_4,\,in} + 3 \times F_{C_2H_6,\,in}} \times 100 \quad (3)$$

3. Results and discussion

3.1. Chemical composition and crystalline structure of SZ-X (X = 0, 1, 2, 3, and 6)

The chemical compositions of SiO_2-ZrO_2 (SZ-*X*) supports determined by SEM–EDS analyses are given in Table 1. The amount of zirconia grafted onto silica increases with the increasing amount of zirconium precursor used from SZ-1 to SZ-6. Nevertheless, the actual zirconium loading is less than that of the zirconium used. This indicates that a considerable amount of the zirconium precursors do not react and is washed out during the preparation step. This is because silica and as-synthesized SiO_2-ZrO_2 supports have a limited number of hydroxyl groups on their surfaces [31]. The Zr/Si atomic ratio of the SZ-*X* supports increases from 0.12 to 1.34 with increasing zirconium loading from 15.4 to 67.1 wt.%.

Table 1
Chemical compositions of SiO_2-ZrO_2 (SZ-*X*) supports determined by SEM–EDS analyses

Support	Amount of Zr used (wt.%)	Actual Zr loading (wt.%)	Zr/Si atomic ratio
SZ-1	20	15.4	0.12
SZ-2	40	32.7	0.39
SZ-3	60	45.1	0.54
SZ-6	120	67.1	1.34

The XRD patterns of commercial Carbosil silica (SZ-0) and SZ-*X* (*X* = 1, 2, 3, and 6) supports calcined at 700 °C are presented in Fig. 2. The SZ-0 and SZ-1 supports show the amorphous diffraction patterns of silica. By contrast, the SZ-*X* (*X* = 2, 3, and 6) supports exhibit diffraction peaks that correspond to the tetragonal phase of zirconia (dashed lines in Fig. 2). The peaks associated with the tetragonal phase of zirconia become narrower and sharper with increasing zirconium content in the SZ-*X* (*X* = 2, 3, and 6) supports, indicating the well-developed zirconia crystalline structure in these supports. The absence of the tetragonal phase of zirconia in SZ-1 is believed to be due to the small amount of zirconia that is finely grafted on the silica surface. The above result suggests that zirconia is successfully grafted on the surface of silica. Compared with SZ-6, SZ-2 and SZ-3 with low zirconium contents (Zr:Si = 0.39 and 0.54, respectively) display relatively broad diffraction patterns that correspond to the tetragonal phase of zirconia, indicating that zirconia is finely dispersed in the SZ-2 and SZ-3 supports. It is believed that the co-existence of ZrO_2 and SiO_2 components stabilized the surface structure of the SiO_2-ZrO_2 composite support prepared by a grafting method.

Another noticeable point is that SZ-6 shows not only a tetragonal phase (majority) but also a monoclinic phase (minority) of zirconia. It has been reported that the tetragonal phase of zirconia is unstable at room temperature [34] and is transformed to the monoclinic phase at high temperatures [33]. Such a phase transformation may be understood by the size effect. When the

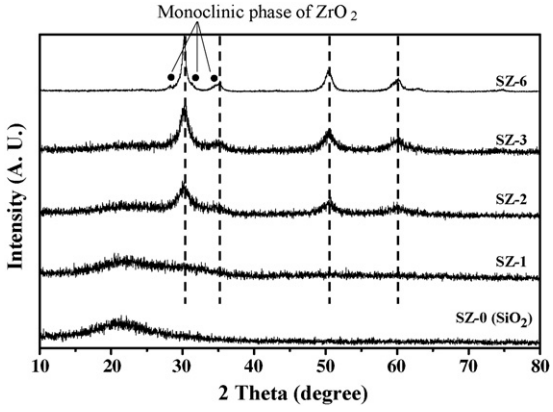

Fig. 2. XRD patterns of commercial Carbosil silica (SZ-0) and SZ-*X* (*X* = 1, 2, 3, and 6) supports calcined at 700 °C. Dashed lines represent tetragonal phase of zirconia.

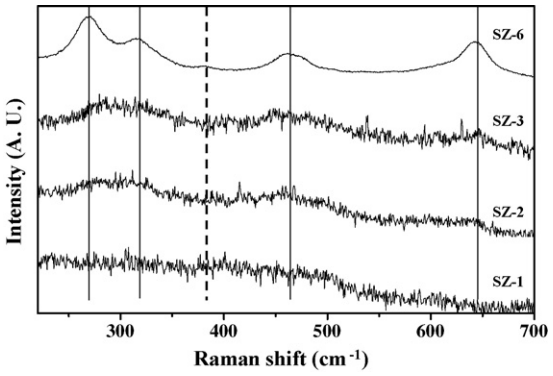

Fig. 3. Raman spectra of SZ-*X* (*X* = 1, 2, 3, and 6). Solid lines represent tetragonal phase of zirconia and dashed line represents monoclinic phase of zirconia.

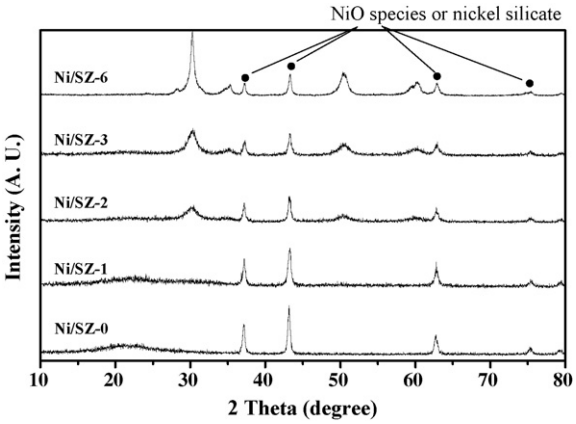

Fig. 4. XRD patterns of Ni/SZ-*X* (*X* = 0, 1, 2, 3, and 6) catalysts calcined at 700 °C for 5 h.

grain size of zirconia exceeds a critical value, phase transformation from the tetragonal phase to the monoclinic phase can occur [33]. It should be noted that the size of zirconia in SZ-6 is larger than that in the other supports, and this leads to a phase transformation from the tetragonal phase to the monoclinic phase in the SZ-6 support. The above results imply that the crystalline structures of the SZ-*X* supports are strongly influenced by the amount of zirconia grafted.

It would be expected that the stabilizing effect achieved through the formation of a SiO_2-ZrO_2 composite structure is not dominant in the SZ-6. This is well confirmed by Raman spectroscopy analyses. The Raman spectra of SZ-*X* (*X* = 1, 2, 3, and 6) exhibit no distinguishable peaks corresponding to the active mode of ZrO_2 (see Fig. 3). On the other hand, SZ-2 and SZ-3 have broad and weak peaks corresponding to the typical active mode of the tetragonal phase of ZrO_2 (solid lines in Fig. 3) [33]. It is believed that the SiO_2-ZrO_2 composite structure inhibits the growth of crystalline ZrO_2 in the SZ-*X* (*X* = 1, 2, and 3) supports. By contrast, SZ-6 shows relatively sharp peaks corresponding to the active modes of the tetragonal phase of ZrO_2 (solid lines in Fig. 3) and a weak peak corresponding to the monoclinic phase (dashed line in Fig. 3) [33]. These results are in good agreement with the XRD results given in Fig. 2. It is concluded that the excess amount of zirconia grafted on the silica in the SZ-6 support causes a weak interaction between SiO_2 and ZrO_2.

3.2. Crystalline structure of Ni/SZ-X (X = 0, 1, 2, 3, and 6)

The XRD patterns of Ni/SZ-*X* (*X* = 0, 1, 2, 3, and 6) catalysts calcined at 700 °C for 5 h are presented in Fig. 4. All of the prepared catalysts display diffraction peaks for NiO (JCPDS 22-1189) and nickel silicate species. It is difficult to distinguish between these species due to the overlap of the XRD peaks. The particle size of the nickel oxide species, calculated using the Scherrer equation at $2\theta = 75.3°$, decreases in the order: Ni/SZ-0 (38.7 nm) > Ni/SZ-6 (37.9 nm) > Ni/SZ-1 (36.4 nm) > Ni/SZ-2 (34.9 nm) > Ni/SZ-3 (32.7 nm). It is well known that the particle size of NiO species and their dispersion on the support are strongly influenced by metal–support interactions. For example, Ni^{2+} is incorporated into the matrix of alumina to form nickel aluminate at high calcination temperatures, leading to strong interactions between nickel and alumina in the Ni/Al_2O_3 catalyst [34,35]. The strong interaction between metal and support increases the dispersion of NiO species and decreases the particle size of the NiO species. The crystalline structures of the Ni/SZ-*X* (*X* = 0, 1, 2, 3, and 6) catalysts prepared in this work are also influenced by metal–support interactions. It has been suggested [15] that the grafted zirconia enhances nickel–support interactions through the formation of a SiO_2-ZrO_2 composite structure. It is also known that zirconia acts as a promoter, similar to MgO and CeO_2, to prevent the formation of large nickel oxide species [12,15]. Therefore, it is believed that zirconia serves as a spacer or a barrier and prevents the formation of large nickel oxide species during the calcination process [12,36]. Except for Ni/SZ-6, the particle size of the nickel oxide species decreases with increasing zirconium content. In the case of Ni/SZ-6, however, it is likely that nickel is supported not only on the surface of the SiO_2-ZrO_2 composite but also on the outer surface of the zirconia, judging from the fact that the stabilizing effect achieved through the formation of a SiO_2-ZrO_2 composite structure is not dominant in the SZ-6 (Figs. 2 and 3), which is due to the use of an excess amount of zirconia (Zr/Si = 1.34) in the preparation of SZ-6. The relatively weak interaction between the nickel oxide species and zirconia is also responsible for the decreased dispersion and increased particle size of the nickel oxide species in the Ni/SZ-6.

3.3. Reducibility of Ni/SZ-X (X = 0, 1, 2, 3, and 6)

TPR measurements were carried out to investigate the reducibility of the Ni/SZ-*X* (*X* = 0, 1, 2, 3, and 6) catalysts and to examine the interaction between nickel species and SZ-*X* (*X* = 0, 1, 2, 3, and 6) supports. Fig. 5 shows the TPR profiles of Ni/SZ-*X* (*X* = 0, 1, 2, 3, and 6) catalysts. The Ni/SZ-0 catalyst exhibits a broad reduction peak at around 500 °C, which indicates a weak interaction between the nickel oxide species and the silica support. The reduction peak of Ni/SZ-*X* (*X* = 1, 2, and 3) shifts to higher temperature with increasing zirconium content. This indicates that the grafted zirconia increases the interaction between the nickel oxide species and the support through the formation of a SiO_2-ZrO_2 composite structure with increasing zirconium

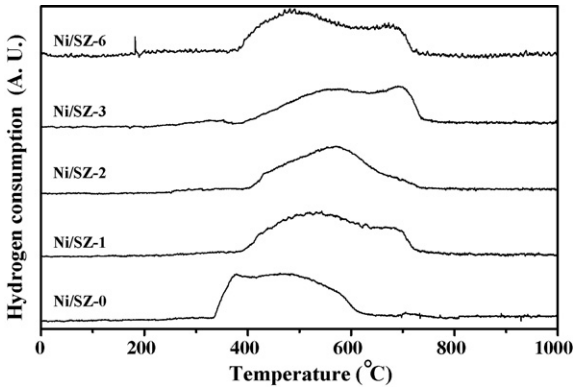

Fig. 5. TPR profiles of Ni/SZ-*X* (*X* = 0, 1, 2, 3, and 6) catalysts.

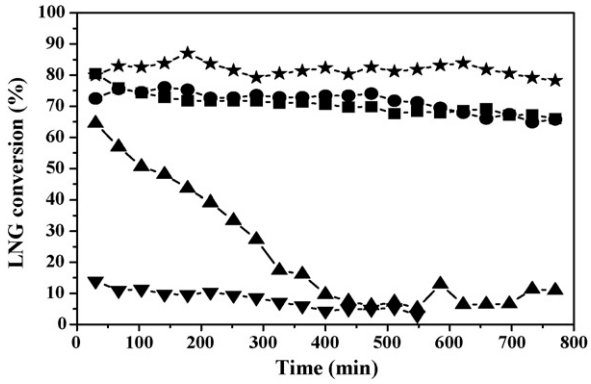

Fig. 6. LNG conversion with time on stream in steam reforming of LNG over Ni/SZ-*X* (*X* = 0, 1, 2, 3, and 6) catalysts at 600 °C (▼, Ni/AZ-0; ▲, Ni/AZ-1; ●, Ni/AZ-2; ⋆, Ni/AZ-3; ■, Ni/AZ-6).

content, resulting in the poor reducibility of Ni/SZ-*X* (*X* = 1, 2, and 3) with increasing zirconium content. It is also likely that the grafted zirconia may enhance the incorporation of Ni^{2+} into the silica matrix, resulting in the formation of highly dispersed nickel silicate species [15]. It is believed that the reduction band at around 600 °C in the Ni/SZ-*X* (*X* = 1, 2, and 3) can be attributed to the reduction of nickel oxide species that have strongly interacted with the support, while the reduction band at around 700 °C might be due to the reduction of nickel silicate species [15,37].

On the other hand, Ni/SZ-6 shows lower reduction peak temperatures than Ni/SZ-*X* (*X* = 1, 2, and 3). The reduction band at around 500 °C is thought to be due to the reduction of nickel oxide species that have interacted weakly with zirconia [37]. As mentioned above, an excess amount of zirconia grafted on the silica in the SZ-6 would cause a weak interaction between SiO_2 and ZrO_2, and nickel would be supported not only on the SiO_2-ZrO_2 composite support but also on the zirconia. The reduction band at around 700 °C in the Ni/SZ-6 is attributed to nickel silicate species on the SiO_2-ZrO_2 composite support, as is observed for Ni/SZ-*X* (*X* = 1, 2, and 3). Among the supported catalysts, the Ni/SZ-3 has the poorest reducibility due to the fine dispersion of nickel oxide species on the SiO_2-ZrO_2 support and the strong interaction of nickel oxide species with the SiO_2-ZrO_2 support.

3.4. Steam reforming of LNG over Ni/SZ-X (X = 0, 1, 2, 3, and 6) catalysts

Fig. 6 shows LNG conversion with time on stream in the steam reforming of LNG over Ni/SZ-*X* (*X* = 0, 1, 2, 3, and 6) catalysts at 600 °C. The Ni/SZ-0 gives a low LNG conversion during the reaction period, and a significant catalyst deactivation occurs. Although the Ni/SZ-0 catalyst retains nickel oxide species that interact weakly with silica (Fig. 5), the poor resistance of silica to steam and the sintering of nickel particles result from weak interaction between nickel and silica in the oxidation atmosphere (in the presence of steam), and cause significant catalyst deactivation of Ni/SZ-0 [15]. Ni/SZ-1 produces a higher LNG conversion than Ni/SZ-0, but it experiences severe catalyst deactivation. Although the addition of zirconia enhances the resistance of silica to steam and increases the resistance against sintering of nickel particles, it appears that the content of zirconia in Ni/SZ-1 is not sufficient to play such a role. On the other hand, Ni/SZ-*X* (*X* = 2, 3, and 6) gives a stable and high catalytic performance during a catalytic reaction that extends over 800 min. It can be inferred that a critical amount of zirconia is required in the Ni/SZ-*X* catalysts for efficient steam reforming of LNG.

The LNG conversion is decreased in the order: Ni/SZ-3 (Zr/Si = 0.54) > Ni/SZ-2 (Zr/Si = 0.39) > Ni/SZ-6 (Zr/Si = 1.34) > Ni/SZ-1 (Zr/Si = 0.12) > Ni/SZ-0 (Zr/Si = 0). Among the catalysts tested, the Ni/SZ-3 gives the highest LNG conversion. This can be explained by the effect of zirconia grafted on the surface of silica. One possible reason for this is the fine dispersion of nickel particles in the Ni/SZ-3 catalyst. Although catalyst reducibility is not the sole determining factor for catalytic performance, the poor reducibility of Ni/SZ-3 implies that nickel particles were finely dispersed on the support (Fig. 5) due to the strong interaction between the nickel species and the support. Under our reduction conditions performed at 800 °C, however, Ni/SZ-3 with the poorest reducibility can be reduced completely. Therefore, reducibility does not serve as a critical factor determining the catalytic performance in our reaction system. It is concluded that nickel particle size plays an important role in determining the catalytic performance in the steam reforming of LNG over the Ni/SZ-*X* catalysts. It is likely that the optimum atomic ratio of Zr/Si in the Ni/SZ-3 catalyst favourably alters the interaction between nickel species and support, making it more suitable for the steam reforming of LNG. Another possible reason for the enhanced catalytic performance of Ni/SZ-3 is the presence of highly dispersed zirconia on the silica surface. This prevents the growth of nickel oxide species during the calcination process through the formation of a ZrO_2-SiO_2 support with a favourable structure (Fig. 4). Zirconia is known to have a high capacity for steam adsorption. It is believed that the zirconia in our catalyst system also plays a role in enhancing the spillover of adsorbed steam from the support to the active nickel [24]. The migrated steam, in turn, enhances the gasification of surface hydrocarbons, which results in an enhancement of both LNG conversion and hydrogen yield. It appears that the well-developed and pure tetragonal phase of SZ-3 (Fig. 2) plays an important role in the adsorption of steam and subsequent spillover of steam from the support to the active nickel.

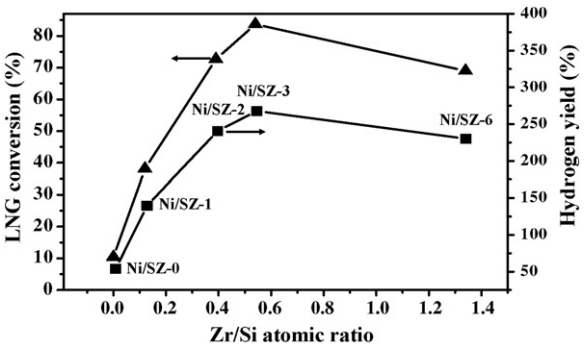

Fig. 7. LNG conversion and hydrogen yield as function of Zr/Si atomic ratio over Ni/SZ-*X* (*X* = 0, 1, 2, 3, and 6) catalysts in steam reforming of LNG at 600 °C. Data obtained after a reaction of 200 min.

The LNG conversion and hydrogen yield is shown in Fig. 7 as a function of Zr/Si atomic ratio over Ni/SZ-*X* (*X* = 0, 1, 2, 3, and 6) catalysts in the steam reforming of LNG at 600 °C. The data are obtained after a reaction of 200 min and reveal that LNG conversion and hydrogen yield have volcano-shaped curves with respect to the Zr/Si atomic ratio. Both LNG conversion and hydrogen yield decrease in the order: Ni/SZ-3 (Zr/Si = 0.54) > Ni/SZ-2 (Zr/Si = 0.39) > Ni/SZ-6 (Zr/Si = 1.34) > Ni/SZ-1 (Zr/Si = 0.12) > Ni/SZ-0 (Zr/Si = 0). Among the catalysts tested, the Ni/SZ-3 catalyst exhibits the best catalytic performance. These results imply that an optimum ratio of Zr/Si is required for the maximum production of hydrogen by steam reforming of LNG.

3.5. Crystalline structure of used Ni/SZ-X (X = 0, 1, 2, 3, and 6)

The XRD patterns of Ni/SZ-*X* (*X* = 0, 1, 2, 3, and 6) catalysts obtained after a reaction at 600 °C for 800 min are presented in Fig. 8. All the Ni/SZ-*X* (*X* = 0, 1, 2, 3, and 6) catalysts display diffraction peaks for metallic nickel (JCPDS 03-1051). Interestingly, Ni/SZ-0 also exhibits small diffraction peaks for NiO species. This suggests that the weakly supported metallic nickel is oxidized by the coarsening of silica as a result of its poor steam resistance. The Ni/SZ-1 has the largest particle size of metallic nickel (48 nm). This indicates that the aggregation of weakly supported metallic nickel is accelerated by the coalescence of the SZ-1 support due to its insufficient resistance to steam. This is the reason why the Ni/SZ-1 has a lower catalytic activity than the Ni/SZ-6, although the calcined Ni/SZ-1 retains a smaller particle size of nickel oxide species than the Ni/SZ-6. Among the catalysts, Ni/SZ-3 has the smallest particle size of metallic nickel (35 nm). It is believed that the Ni/SZ-3 retains an optimum atomic ratio of Zr/Si for effective retardation of the sintering of metallic nickel particles during the reaction, by forming a favourable SiO_2-ZrO_2 composite structure.

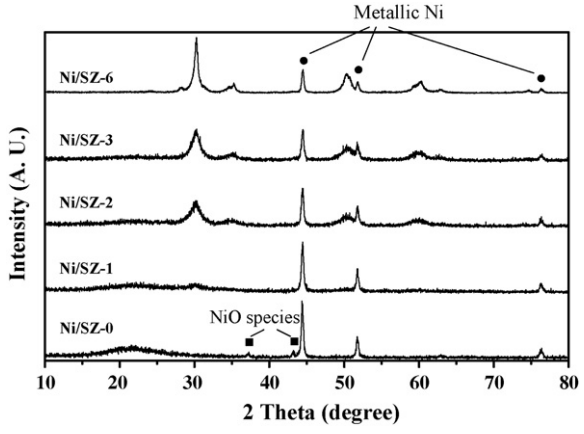

Fig. 8. XRD patterns of Ni/SZ-*X* (*X* = 0, 1, 2, 3, and 6) catalysts obtained after reaction at 600 °C for 800 min.

4. Conclusions

A series of SiO_2-ZrO_2 (SZ-*X*) supports with various zirconium contents have been prepared by grafting a zirconium precursor onto the surface of Carbosil silica. Ni/SiO_2-ZrO_2 catalysts have then been prepared by an impregnation method for use in hydrogen production by steam reforming of LNG. The effect of SiO_2-ZrO_2 supports on the performance of the Ni/SiO_2-ZrO_2 catalysts has been investigated. It is found that zirconia markedly enhances the resistance of silica to steam and increases the interaction between the nickel and the support. It also prevents the growth of nickel oxide species during the calcination process through the formation of a ZrO_2-SiO_2 composite structure. The crystalline structures and catalytic activities of the Ni/SZ-*X* catalysts are strongly influenced by the amount of zirconium grafted. In hydrogen production by steam reforming of LNG, both LNG conversion and the hydrogen yield show volcano-shaped curves with respect to the Zr/Si atomic ratio. Both LNG conversion and hydrogen yield decrease in the order: Ni/SZ-3 (Zr/Si = 0.54) > Ni/SZ-2 (Zr/Si = 0.39) > Ni/SZ-6 (Zr/Si = 1.34) > Ni/SZ-1 (Zr/Si = 0.12) > Ni/SZ-0 (Zr/Si = 0). Among the catalysts tested, the Ni/SZ-3 catalyst exhibits the best catalytic performance. The well-developed and pure tetragonal phase of SZ-3 plays an important role in the adsorption of steam and the subsequent spillover of steam from the support to the active nickel. The small particle size of the metallic nickel in the Ni/SZ-3 is also responsible for its high catalytic performance. It is concluded that SiO_2-ZrO_2 (SZ-*X*) prepared by a grafting method can serve as an efficient support for the nickel catalyst in hydrogen production by steam reforming of LNG, and that an optimum ratio of Zr/Si is required for the maximum performance of Ni/SZ-*X* catalysts.

Acknowledgements

The authors wish to acknowledge support from the Seoul Renewable Energy Research Consortium (Seoul R & BD Program) and RCECS (Research Center for Energy Conversion and Storage: R11-2002-102-00000-0).

References

[1] M. Schrope, Nature 414 (2001) 682.
[2] B. Darren, J. Power Sources 65 (1997) 128.
[3] Y.H. Wang, Adv. Environ. Sci. 1 (1999) 172.

[4] J.N. Armor, Appl. Catal. A 176 (1999) 159.
[5] K.J. Lee, D. Park, Korean J. Chem. Eng. 15 (1998) 658.
[6] K.D. Ko, J.K. Lee, D. Park, S.H. Shin, Korean J. Chem. Eng. 12 (1995) 478.
[7] S.W. Nahm, S.P. Youn, H.Y. Ha, S.-A. Hong, A.P. Maganyuk, Korean J. Chem. Eng. 17 (2000) 288.
[8] Q. Ming, T. Healey, L. Allen, P. Irving, Catal. Today 77 (2002) 51.
[9] J. Sehested, J.A.P. Gelten, I.N. Remediakis, H. Bengaard, J.K. Nørskov, J. Catal. 223 (2004) 432.
[10] T. Borowiecki, G. Wojciech, D. Andrzej, Appl. Catal. A 270 (2004) 27.
[11] J.S. Lisboa, D.C.R.M. Santos, F.B. Passos, F.B. Noronha, Catal. Today 101 (2005) 15.
[12] S. Natesakhawat, R.B. Watson, X. Wang, U.S. Ozkan, J. Catal. 234 (2005) 496.
[13] M.E.S. Hegarty, A.M. O'Connor, J.R.H. Ross, Catal. Today 42 (1998) 225.
[14] H.-S. Roh, K.-W. Jun, S.-E. Park, Appl. Catal. A 251 (2003) 275.
[15] R. Takahashi, S. Sato, T. Sodesawa, M. Yoshida, S. Tomiyama, Appl. Catal. A 273 (2004) 211.
[16] E. Ruckenstein, Y.H. Hu, J. Catal. 162 (1996) 230.
[17] M.A. Keane, J. Catal 166 (1997) 347.
[18] D. Klvana, J. Chaouki, D. Kusohorosky, C. Chavarie, G. Pajonk, Appl. Catal. 42 (1998) 121.
[19] J. Kim, D.J. Suh, T.J. Park, K. Ki, Appl. Catal. A 197 (2000) 191.
[20] L. Larner, K. Speakman, A. Majumdar, J. Non-Cryst. Solids 20 (1976) 43.
[21] K. Kamiya, S. Sakka, Y. Tatemichi, J. Mater. Sci. 15 (1980) 1765.
[22] T. Yazawa, A. Miyake, H. Tanaka, J. Ceram. Soc. Jpn. 99 (1991) 1094.
[23] Y. Tsurita, M. Nogami, J. Ceram. Soc. Jpn. 109 (2001) 992.
[24] Y. Matsumura, T. Nakamori, Appl. Catal. A 258 (2004) 107.
[25] A. Tarafdar, A.B. Panda, P. Pramanik, Microporous Mesoporous Mater. 84 (2005) 223.
[26] Z.-G. Wu, Y.-X. Zhao, D.-S. Liu, Microporous Mesoporous Mater. 68 (2004) 127.
[27] C. Flego, L. Carluccio, C. Rizzo, C. Perego, Catal. Commun. 2 (2001) 43.
[28] Z. Dang, B.G. Anderson, Y. Amenomiya, B.A. Morrow, J. Phys. Chem. 99 (1995) 14437.
[29] C.I. Odenbrand, S. Andersson, L. Andersson, J. Brandin, G. Busca, J. Catal. 125 (1990) 541.
[30] H. Chen, J. Gao, M. Ruan, J. Shi, D. Yan, Microporous Mesoporous Mater. 76 (2004) 209.
[31] P. Iengo, M.D. Serio, V. Solinas, D. Gazzoli, G. Salvio, E. Santacesaria, Appl. Catal. A 170 (1998) 225.
[32] T. Yamaguchi, Catal. Today 20 (1994) 199.
[33] T. Klimova, M.L. Rojas, P. Castillo, R. Cuevas, Microporous Mesoporous Mater. 20 (1998) 293.
[34] P. Kim, Y. Kim, H. Kim, I.K. Song, J. Yi, Appl. Catal. A 272 (2004) 157.
[35] P. Kim, Y. Kim, H. Kim, I.K. Song, J. Yi, J. Mol. Catal. A 231 (2005) 247.
[36] M.H. Youn, J.G. Seo, P. Kim, J.J. Kim, H.-I. Lee, I.K. Song, J. Power Sources 162 (2006) 1270.
[37] G. Goncalves, M.K. Lenzi, Q.A.A. Santos, L.M.M. Jorge, J. Non-Cryst. Solids 352 (2006) 3697.